

# Nucleon Charges from 2+1+1-flavor HISQ and 2+1-flavor clover lattices

**Rajan Gupta**<sup>\*†</sup>

*Los Alamos National Laboratory, Los Alamos, NM, 87545, U.S.A.*

*E-mail:* [rajan@lanl.gov](mailto:rajan@lanl.gov)

**PNDME and NME Collaborations**<sup>‡</sup>

Precise estimates of the nucleon charges  $g_A$ ,  $g_S$  and  $g_T$  are needed in many phenomenological analyses of SM and BSM physics. In this talk, we present results from two sets of calculations using clover fermions on 9 ensembles of 2+1+1-flavor HISQ and 4 ensembles of 2+1-flavor clover lattices. We show that high statistics can be obtained cost-effectively using the truncated solver method with bias correction and the coherent source sequential propagator technique. By performing simulations at 4–5 values of the source-sink separation  $t_{\text{sep}}$ , we demonstrate control over excited-state contamination using 2- and 3-state fits. Using the high-precision 2+1+1-flavor data, we perform a simultaneous fit in  $a$ ,  $M_\pi$  and  $M_\pi L$  to obtain our final results for the charges.

*34th annual International Symposium on Lattice Field Theory*

*24-30 July 2016*

*University of Southampton, UK*

---

<sup>\*</sup>Speaker.

<sup>†</sup>LA-UR-16-29008

<sup>‡</sup>Calculations on the 2+1+1-flavor HISQ lattices are being done in collaboration with T. Bhattacharya, V. Cirigliano, Y. C. Jang, H-W. Lin and B. Yoon. Calculations on the 2+1-clover ensembles are being done in collaboration with T. Bhattacharya, V. Cirigliano, J. Green, Bálint Joó, Y. C. Jang, H-W. Lin, K. Orginos, D. Richards, S. Syritsen, F. Winter and B. Yoon.

## 1. Introduction

In this talk, we highlight three areas in which significant progress has been made to extract matrix elements of quark bilinear operators within nucleon states. (i) cost-effective increase of statistics using the truncated solver method with bias correction and the coherent source sequential propagator technique; (ii) inclusion of up to 4-states (3-states) in the analysis of 2-point (3-point) correlation functions; and (iii) a simultaneous fit in  $a$ ,  $M_\pi$  and  $M_\pi L$  to data at different  $a$ ,  $M_\pi$  and  $L$  to get the physical value. The results presented here are based on Refs. [10, 3, 11]. A summary of the lattice ensembles used and measurements made in the clover-on-HISQ study is given in Table 1 and in the clover-on-clover study in Table 2. Associated results for the isovector form factors:  $G_E(q^2)$ ,  $G_M(q^2)$ ,  $G_A(q^2)$ , and  $G_S^s(Q^2)$  were presented by Yong-Chull Jang at this conference [8].

## 2. Increasing Statistics Cost-effectively

The various systematic uncertainties in the calculation of matrix elements (ME) of local quark bilinear operators within nucleon states are at the 5% level [3]. In order to isolate, understand and address these systematics, one needs data with statistical errors that are significantly smaller. To reduce statistical errors, one needs to make measurements on significant numbers of decorrelated lattices that adequately importance sample the phase space of the path integral. We have found the following three techniques to be cost-effective ways of reducing the statistical errors.

Lattices with  $M_\pi L \geq 4$  can be regarded as consisting of a large number of uncorrelated regions, i.e., measurements of nucleon correlation functions in different sub-regions are statistically uncorrelated. Since the generation of lattices with dynamical fermions is expensive, one should assess the dimensions of these sub-regions. For ME within nucleon states we find that  $O(100)$  measurements per lattice of size  $M_\pi L = 4$  are cost-effective [10]. Furthermore, choosing the source points randomly within these sub-regions of a lattice and between lattices reduces correlations.

Computer time can be reduced significantly by using the coherent source sequential propagator method [10]. For example, if  $N_{\text{meas}}$  measurements on a given lattice are done in a single computer job, then the number of quark propagators that need to be calculated using coherent sources reduces to  $N_{\text{meas}} + 2$  from  $N_{\text{meas}} + 2 \times N_{\text{meas}}$  in the standard approach.

Lastly, in a given measurement, one has the freedom to choose the precision with which quark propagators are calculated. The truncated solver method [1] with bias correction [5] significantly reduces the computational time. In Ref. [3], we show that a stopping residue  $r_{\text{LP}} \equiv |\text{residue}|_{\text{LP}}/|\text{source}| = 10^{-3}$  reduces cost by a factor of about 17 compared to  $r_{\text{HP}} = 10^{-10}$ . Possible bias is corrected for using

$$C^{\text{imp}} = \frac{1}{N_{\text{LP}}} \sum_{i=1}^{N_{\text{LP}}} C_{\text{LP}}(\mathbf{x}_i^{\text{LP}}) + \frac{1}{N_{\text{HP}}} \sum_{i=1}^{N_{\text{HP}}} [C_{\text{HP}}(\mathbf{x}_i^{\text{HP}}) - C_{\text{LP}}(\mathbf{x}_i^{\text{HP}})] ,$$

where  $C_{\text{LP}}$  and  $C_{\text{HP}}$  are the 2- and 3-point correlation functions calculated in low- (LP) and high-precision (HP), respectively, and  $\mathbf{x}_i^{\text{LP}}$  and  $\mathbf{x}_i^{\text{HP}}$  are the two kinds of source positions. Bias, given by the second term, if present, was much smaller than the statistical errors. Speedup is achieved because we need 1 HP and LP measurement for bias correction for every 32 LP used for statistics.

Ensemble ID	$a$ (fm)	$M_\pi^{\text{sea}}$ (MeV)	$M_\pi^{\text{val}}$ (MeV)	$L^3 \times T$	$M_\pi^{\text{val}} L$	$N_{\text{conf}}$	$N_{\text{meas}}^{\text{HP}}$	$N_{\text{meas}}^{\text{AMA}}$
a12m310	0.1207(11)	305.3(4)	310(3)	$24^3 \times 64$	4.55	1013	8104	64832
a12m220S	0.1202(12)	218.1(4)	225(2)	$24^3 \times 64$	3.29	1000	24000	
a12m220	0.1184(10)	216.9(2)	228(2)	$32^3 \times 64$	4.38	958	7664	
a12m220L	0.1189(9)	217.0(2)	228(2)	$40^3 \times 64$	5.49	1010	8080	68680
a09m310	0.0888(8)	312.7(6)	313(3)	$32^3 \times 96$	4.51	881	7048	
a09m220	0.0872(7)	220.3(2)	226(2)	$48^3 \times 96$	4.79	890	7120	
a09m130	0.0871(6)	128.2(1)	138(1)	$64^3 \times 96$	3.90	883	7064	84768
a06m310	0.0582(4)	319.3(5)	320(2)	$48^3 \times 144$	4.52	1000	8000	64000
a06m220	0.0578(4)	229.2(4)	235(2)	$64^3 \times 144$	4.41	650	2600	41600
a06m135	0.0568(1)	135.5(2)	136(2)	$96^3 \times 192$	3.74	229	1145	36640

Table 1: Summary of the ensembles used in the clover-on-HISQ study. For the a06m130 ensemble, preliminary results on form factors only were presented by Y-P Jang at this conference.

Ensemble ID	$a$ (fm)	$M_\pi^{\text{sea}}$ (MeV)	$L^3 \times T$	$M_\pi^{\text{val}} L$	$N_{\text{conf}}$	$N_{\text{meas}}^{\text{HP}}$	$N_{\text{meas}}^{\text{AMA}}$
a127m285	0.127(2)	285(3)	$32^3 \times 96$	5.85	1000	4020	128480
a094m280	0.094(1)	278(3)	$32^3 \times 64$	4.11	1005	3015	96480
a091m170	0.091(1)	166(2)	$48^3 \times 96$	3.7	629	2516	80512
a091m170L	0.091(1)	172(6)	$64^3 \times 128$	5.08	467	2335	74720

Table 2: Summary of the ensembles used in the clover-on-HISQ study. Here  $M_\pi^{\text{sea}} = M_\pi^{\text{val}}$

### 3. Reducing Systematic Uncertainties

The above techniques allowed us to make, on each ensemble,  $O(10^5)$  measurements on  $O(1000)$  lattices. In these measurements of 2- and 3-point correlation functions, two systematics need to be addressed in order to extract the charges, form factors, and other ME: removing excited-state contamination (ESC) and precise determination of the renormalization factor connecting the lattice operator to some phenomenological scheme such as the  $\overline{\text{MS}}$  scheme at  $\mu = 2 \text{ GeV}$ .

ESC arises because typical interpolating operators used to create and annihilate meson and baryon states on the lattice couple to the ground state, all its excitations and multiparticle states with the same quantum numbers. Thus, contributions of all higher states have to be removed to obtain the desired ME within the ground state. The behavior of the 2- and 3-point correlation functions, given by the spectral decomposition, has contributions from a tower of intermediate states in terms of unknown amplitudes  $\mathcal{A}_i$ , energies  $M_i$  and ME  $\langle f | \mathcal{O}_\Gamma | i \rangle$  that are extracted from fits. Formally, the ground state ME  $\langle 0 | \mathcal{O}_\Gamma | 0 \rangle$  can be obtained by calculating the 3-point functions with very large source-sink separation  $t_{\text{sep}}$ . For baryons, the signal in 2- and 3-point function degrades exponentially, and for values of  $t_{\text{sep}}$  accessible with  $O(10^5)$  measurements, the ESC is found to be significant. Thus, methods to minimize ESC in calculations with  $1 \lesssim t_{\text{sep}} \lesssim 1.5 \text{ fm}$  are needed.

We demonstrate control over ESC by (i) constructing the interpolating operators using tuned

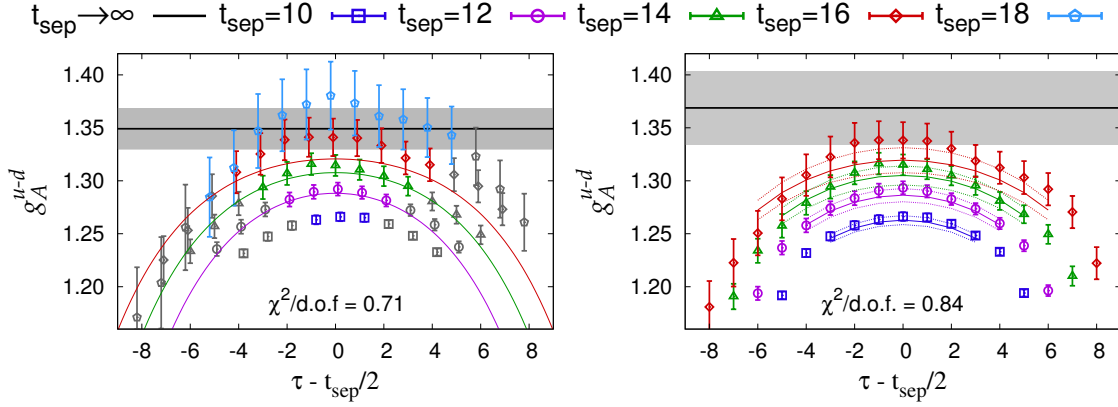


Figure 1: Unrenormalized  $g_A^{u-d}$  on the  $a081m315$  2+1-flavor clover ensemble with  $\sigma = 5$  smearing. The left (right) panel shows the data, 2-state (3-state) fit, and  $t_{\text{sep}} \rightarrow \infty$  estimate (grey band).

smearing sources in the generation of the quark propagators; (ii) performing the calculation at multiple values of  $t_{\text{sep}}$ ; (iii) inserting the operator at all intermediate timeslices  $\tau$  between the source and sink; (iv) analyzing the 2- and 3-point correlators by including increasing number of intermediate states. For example, the 2-state truncation of the zero-momentum correlation functions is

$$C^{2\text{pt}}(t_f, t_i) = |\mathcal{A}_0|^2 e^{-M_0(t_f - t_i)} + |\mathcal{A}_1|^2 e^{-M_1(t_f - t_i)}, \quad (3.1)$$

$$C_{\Gamma}^{3\text{pt}}(t_f, \tau, t_i) = |\mathcal{A}_0|^2 \langle 0 | \mathcal{O}_{\Gamma} | 0 \rangle e^{-M_0(t_f - t_i)} + |\mathcal{A}_1|^2 \langle 1 | \mathcal{O}_{\Gamma} | 1 \rangle e^{-M_1(t_f - t_i)} + \mathcal{A}_0 \mathcal{A}_1^* \langle 0 | \mathcal{O}_{\Gamma} | 1 \rangle e^{-M_0(\tau - t_i)} e^{-M_1(t_f - \tau)} + \mathcal{A}_0^* \mathcal{A}_1 \langle 1 | \mathcal{O}_{\Gamma} | 0 \rangle e^{-M_1(\tau - t_i)} e^{-M_0(t_f - \tau)}, \quad (3.2)$$

where  $\tau$  is the operator insertion time and  $t_f - t_i = t_{\text{sep}}$  in the 3-point function calculation. The states  $|0\rangle$  and  $|1\rangle$  represent the ground and “first excited” nucleon states, respectively. In 2-state analysis, the four parameters,  $M_0$ ,  $M_1$ ,  $\mathcal{A}_0$  and  $\mathcal{A}_1$  are estimated first from fits to the 2-point data and then used as input in fits to 3-point functions to obtain the three ME  $\langle 0 | \mathcal{O}_{\Gamma} | 0 \rangle$ ,  $\langle 0 | \mathcal{O}_{\Gamma} | 1 \rangle$  and  $\langle 1 | \mathcal{O}_{\Gamma} | 1 \rangle$ . The estimate of the charge  $g_{\Gamma} = \langle 0 | \mathcal{O}_{\Gamma} | 0 \rangle$  improves with number of  $t_{\text{sep}}$ , the precision of the data, and the number of states included in the fits. We find that with  $O(10^5)$  measurements, fits with 4 states (3 states) to the 2-point (3 point) functions with full covariance matrix can be made. Stable and consistent estimates of the charges in the  $t_{\text{sep}} \rightarrow \infty$  limit are obtained using data with 4–5 values of  $t_{\text{sep}}$  in the range 1–1.5 fm. A comparison of the 2- and 3-state fits, and the consistency of the  $t_{\text{sep}} \rightarrow \infty$  value obtained for the isovector axial charge  $g_A^{u-d}$  is illustrated in Fig. 1.

Results for the various ME are then renormalized by multiplicative factors  $Z_{\Gamma}$  calculated using the RI-sMOM scheme as discussed in Ref. [3]. Errors in the ME and  $Z_{\Gamma}$  are combined in quadratures. This gives us a set of renormalized lattice estimates as functions of  $a$ ,  $M_{\pi}$  and  $M_{\pi}L$ .

#### 4. Simultaneous fit in $a$ , $M_{\pi}$ and $M_{\pi}L$

With the renormalized estimates, calculated as functions of  $a$ ,  $M_{\pi}$  and  $M_{\pi}L$ , in hand, results in the limit  $a \rightarrow 0$ ,  $M_{\pi} = 135$  MeV and  $M_{\pi}L \rightarrow \infty$ , are obtained using a simultaneous fit in the three variables. With the current 9 clover-on-HISQ data points, fits are sensitive to only the lowest order

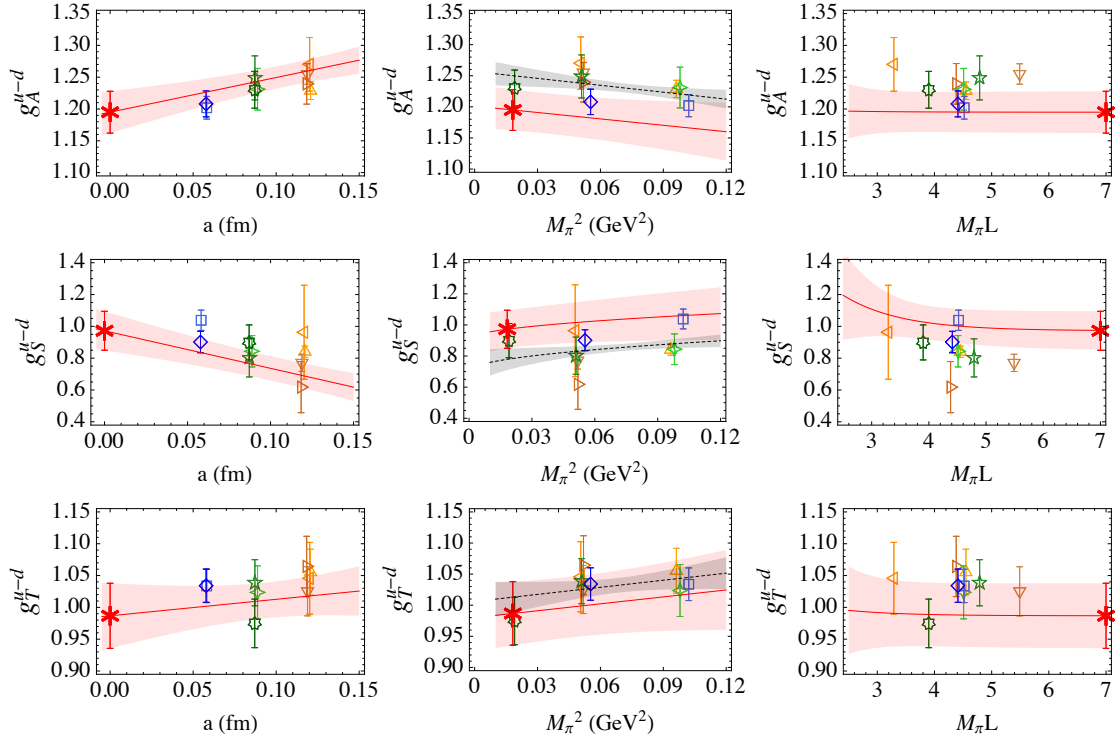


Figure 2: The 9-point fit using Eqs. (4.1) and (4.2) to the data for the renormalized isovector charges,  $g_A^{u-d}$ ,  $g_S^{u-d}$  and  $g_T^{u-d}$ , in the  $\overline{\text{MS}}$  scheme at 2 GeV. The result of the simultaneous extrapolation to the physical point defined by  $a \rightarrow 0$ ,  $M_\pi \rightarrow M_{\pi_0}^{\text{phys}} = 135$  MeV and  $L \rightarrow \infty$  are marked by a red star. The error bands in each panel show the simultaneous fit as a function of a given variable holding the other two at their physical value. The data are shown projected on to each of the three planes. The overlay in the middle figures with the dashed line within the grey band, is the fit to the data versus  $M_\pi^2$  neglecting dependence on the other two variables.

correction terms [3]:

$$g_{A,T}(a, M_\pi, L) = c_1 + c_2 a + c_3 M_\pi^2 + c_4 M_\pi^2 e^{-M_\pi L}, \quad (4.1)$$

$$g_S(a, M_\pi, L) = c_1 + c_2 a + c'_3 M_\pi + c'_4 M_\pi e^{-M_\pi L}. \quad (4.2)$$

Adding next order terms such as chiral logs did not improve the fits (based on the Akaike Information Criteria) and their coefficients were poorly determined. Variation in estimates on including chiral logs were, nevertheless, used to obtain first estimates of the possible systematic uncertainty due to using the lowest order fit ansatz. Our final fits using Eqs. (4.1) and (4.2) are shown in Fig. 2.

The Clover-on-clover estimates on 4 ensembles are consistent with those from clover-on-HISQ at similar values of the lattice parameters. To perform analogous fits to obtain results at  $a \rightarrow 0$  and  $M_\pi = 135$  MeV, clover-on-clover calculations are being extended to additional values of  $a$  and  $M_\pi$ .

## 5. Results: Nucleon Charges to quark EDM

(I) Our results for the isovector nucleon charges, using the simultaneous fit ansatz defined in

Eqs. (4.1) and (4.2) to the 9 clover-on-HISQ data points, are shown in Fig. 2 and give [3]

$$g_A^{u-d} = 1.195(33)(20); \quad g_S^{u-d} = 0.97(12)(6); \quad g_A^{u-d} = 0.987(51)(20). \quad (5.1)$$

(II) Using the conserved vector current relation  $\partial_\mu(\bar{d}\gamma_\mu u) = (m_d - m_u)\bar{d}u$ , lattice estimates of  $m_d - m_u = 2.67(35)$  given by FLAG [9], and our result for  $g_S^{u-d}/g_V^{u-d}$  we obtain

$$(M_N - M_P)^{\text{QCD}} = g_S^{u-d}(m_d - m_u)/g_V^{u-d} = 2.59(49) \text{ MeV}. \quad (5.2)$$

(III) Constraints on novel scalar and tensor couplings,  $\varepsilon_S$  and  $\varepsilon_T$ , at the TeV scale using low-energy experiments and our  $g_S^{u-d}$  and  $g_T^{u-d}$  are derived and compared with those from the LHC in Fig. 3.

(IV) The leading opertors in a low-energy effective theory that contribute to the neutron electric dipole moment (nEDM) are the  $\Theta$ -term, the quark EDM operator and the quark chromo EDM operators. The ME of the quark EDM operator, same as the flavor diagonal tensor charges  $g_T^{u,d,s}$ , are determined to be [2]

$$g_T^u = 0.792(42); \quad g_T^d = -0.194(14); \quad g_T^s = 0.007(8). \quad (5.3)$$

In these estimates, the disconnected contributions to  $g_T^u$  and  $g_T^d$  have been neglected as they were  $O(1\%)$  (smaller than the quoted errors) and poorly determined. Using these results and the experimental bound on the neutron EDM, we performed a first analysis of constraints on possible quark EDM couplings generated at the TeV scale and implications for a split SUSY model in Ref. [2, 4].

## 6. Conclusions and Outlook

Our goal is to calculate the charges and the form factors with  $O(1\%)$  uncertainty on each ensemble and obtain results in the  $a \rightarrow 0$ ,  $M_\pi = 135$  MeV limit with a total error of 2%. This will require simulations with  $O(10^6)$  measurements at 4–5 values of the lattice spacing and on multiple values of the light quark masses close to the physical pion mass. To achieve this goal over the next 5–10 years will require further improvements in algorithms for generating lattices, physics analysis, and the calculation of renormalization factors. Work towards these three goals is ongoing.

## Acknowledgments

We thank the MILC Collaboration for providing the 2+1+1-flavor HISQ ensembles and the JLab/W&M collaboration for the 2+1 clover lattices. Simulations were carried out on computer facilities of (i) Oak Ridge Leadership Computing Facility at the Oak Ridge National Laboratory, which is supported by the Office of Science of the U.S. Department of Energy under Contract No. DE-AC05-00OR22725; (ii) the USQCD Collaboration, which are funded by the Office of Science of the U.S. Department of Energy; (iii) the National Energy Research Scientific Computing Center, a DOE Office of Science User Facility supported by the Office of Science of the U.S. Department of Energy under Contract No. DE-AC02-05CH11231; and (iv) Institutional Computing at Los Alamos National Laboratory; and (v) the Extreme Science and Engineering Discovery Environment (XSEDE), which is supported by the NSF Grant No. ACI-1053575. The calculations used the Chroma software suite [6]. Work supported by the U.S. Department of Energy, NSF and the LANL LDRD program.

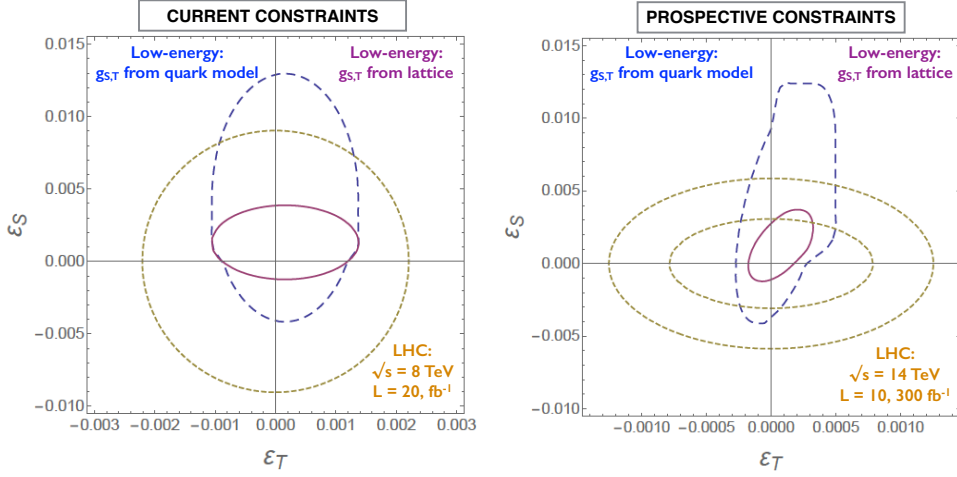


Figure 3: Left panel: current 90% C.L. constraints on  $\epsilon_S$  and  $\epsilon_T$  from beta decays ( $\pi \rightarrow e\nu\gamma$  and  $0^+ \rightarrow 0^+$ ) and the LHC ( $pp \rightarrow e\nu + X$ ) at  $\sqrt{s} = 8$  TeV. Right panel: prospective 90% C.L. constraints on  $\epsilon_S$  and  $\epsilon_T$  from beta decays and the LHC ( $pp \rightarrow e\nu + X$ ) at  $\sqrt{s} = 14$  TeV. The low-energy constraints correspond to  $10^{-3}$  measurements of  $B, b$  in neutron decay and  $b$  in  ${}^6\text{He}$  decay. Both panels present low-energy constraints under two different scenarios for the scalar and tensor charges  $g_{S,T}$ : quark model [7] (large dashed contour) and lattice QCD results given in Eq. (5.1) (small solid contour). LHC constraints are shown as dotted contours.

## References

- [1] Gunnar S. Bali, Sara Collins, and Andreas Schafer. Effective noise reduction techniques for disconnected loops in Lattice QCD. *Comput.Phys.Commun.*, 181:1570–1583, 2010.
- [2] T. Bhattacharya, V. Cirigliano, S. Cohen, R. Gupta, A. Joseph, H-W. Lin, and B. Yoon. Iso-vector and Iso-scalar Tensor Charges of the Nucleon from Lattice QCD. *Phys. Rev.*, D92(9):094511, 2015.
- [3] T. Bhattacharya, V. Cirigliano, S. Cohen, R. Gupta, H-W. Lin, and B. Yoon. Axial, Scalar and Tensor Charges of the Nucleon from 2+1+1-flavor Lattice QCD. *Phys. Rev.*, D94(5):054508, 2016.
- [4] T. Bhattacharya, V. Cirigliano, R. Gupta, H-W. Lin, and B. Yoon. Neutron Electric Dipole Moment and Tensor Charges from Lattice QCD. *Phys. Rev. Lett.*, 115(21):212002, 2015.
- [5] Thomas Blum, Taku Izubuchi, and Eigo Shintani. New class of variance-reduction techniques using lattice symmetries. *Phys.Rev.*, D88(9):094503, 2013.
- [6] Robert G. Edwards and Balint Joo. The Chroma software system for lattice QCD. *Nucl.Phys.Proc.Suppl.*, 140:832, 2005.
- [7] P. Herczeg. Beta decay beyond the standard model. *Prog. Part. Nucl. Phys.*, 46:413–457, 2001.
- [8] Y.C. Jang et al. *ibid*, 2016.
- [9] The Flavor Lattice Averaging Group (FLAG), 2016.
- [10] B. Yoon et al. Controlling Excited-State Contamination in Nucleon Matrix Elements. *Phys. Rev.*, D93(11):114506, 2016.
- [11] B. Yoon et al. Isovector charges of the nucleon from 2+1-flavor QCD with clover fermions, 2016.